

Supporting Information

Preparation and anticancer mechanism of configuration-controlled Fe(II)-Ir(III) heteronuclear metal complexes

Mingxiao Shao, Xicheng Liu*, Yiwei Sun, Shuaihua Dou, Qi Chen, Xiang-Ai Yuan, Laijin Tian, Zhe Liu*

Institute of Anticancer Agents Development and Theranostic Application, The Key Laboratory of Life-Organic Analysis and Key Laboratory of Pharmaceutical Intermediates and Analysis of Natural Medicine, School of Chemistry and Chemical Engineering, Qufu Normal University, Qufu 273165, China.

*Corresponding author, (X. C. Liu) *E-mail*: chemlxc@163.com; Fax: 0086-537-4455228; (Z. Liu) *E-mail*: liuzheqd@163.com, Fax: 0086-537-4455228

1. Experimental section

Materials and Instrumentation: LTRD (Life Technologies, USA), MTDR (Life Technologies, USA), DAPI (Sigma Aldrich, USA), Golgi-Tracker Red (Sigma Aldrich, USA), CCCP (Sigma Aldrich, USA), chloroquine (Sigma Aldrich, USA) and AO (Sigma Aldrich, USA) were used as received. Testing compounds were dissolved in DMSO and diluted with the tissue culture medium before use. Stock solutions of cisplatin (10 mM) and compounds (10 mM) were prepared in DMSO. All stock solutions were stored at -20 °C, thawed and diluted with culture medium prior to each experiment. Note: Chemical reagents and some biological reagents are irritating to the human body. Please pay attention to self-protection.

X-ray Crystallography: All diffraction data were obtained on a Bruker Smart Apex CCD diffractometer equipped with graphite-monochromated Mo K α radiation. Absorption corrections were applied using SADABS program. SQUEEZE option was used to remove the non-localized electron density at the final step of structure refinement. The structures were solved by direct methods using SHELXS (TREF) with additional light atoms found by Fourier methods. Complexes were refined against F_2 using SHELXL, and hydrogen atoms were added at calculated positions and refined riding on their parent atoms. X-ray crystallographic data for **Fe-Ir1** are available as [Tables S1](#) and [S2](#) and deposited in the Cambridge Crystallographic Data Centre under the accession numbers CCDC 1996137.

NMR Spectroscopy: ^1H NMR spectra were acquired in 5 mm NMR tubes at 298 K on Bruker DPX 500 (^1H = 500.13 MHz) spectrometers. ^1H NMR chemical shifts were internally referenced to CHCl_3 (7.26 ppm) for chloroform- d_1 . All data processing was carried out using XWIN-NMR version 3.6 (Bruker UK Ltd.).

UV-vis Spectroscopy: A TU-1901 UV-vis recording spectrophotometer was used with 1 cm path-length quartz cuvettes (3.0 mL). Spectra were processed using UV Winlab software. Experiments were carried out at 298 K unless otherwise stated, and working concentration of DMSO was 0.1% ~ 1% (v/v).

Cell Culture: Human lung epithelial cell (BEAS-2B), human lung cancer cells (A549) and human cervical cancer cells (Hela) were obtained from Shanghai Institute of Biochemistry and Cell Biology (SIBCB). All cell lines were maintained in DMEM media supplemented with fetal bovine serum (10%), and 1% penicillin-streptomycin solution. All cells were grown at 310 K in a humidified incubator under a 5% CO₂ atmosphere.

MTT assay: After plating 5000 A549 cells per well in 96-well plates, the cells were preincubated in drug-free media at 310 K for 24 h before adding different concentrations of compounds to be tested. In order to prepare the stock solution of the drug, the solid complex was dissolved in DMSO and maximum working concentration of DMSO was 1% (v/v). This stock was further diluted using cell culture medium until working concentrations were achieved. The drug exposure period was 24 h. Subsequently, 15 μ L of 5.0 mg mL⁻¹ MTT solution was added to form a purple formazan. Afterwards, 100 μ L of dimethyl sulfoxide (DMSO) was transferred into each well to dissolve the purple formazan, and results were measured using a microplate reader (DNM-9606, Perlong Medical, Beijing, China) at an absorbance of 570 nm. Each well was triplicated and each experiment repeated at least three times. IC₅₀ values quoted are mean \pm SEM.

Measurement of lipophilicity (log*P*_{o/w}): The octanol-water partition coefficients (*P*_{o/w}) of compounds were determined using a shake-flask method. Water (50 mL, distilled after milli-Q purification) and 1-octanol (50 mL, vacuum distilled) were shaken together using a laboratory shaker, for 72 h to allow saturation of both phases. Stock solutions of these compounds (50 μ M) were prepared in the aqueous phase and aliquots (5 mL) of each of these stock solutions were then added to an equal volume of the 1-octanol phase. The resultant biphasic solutions were mixed for 2 h and then centrifuged (3000 \times g, 5 min) to separate the phases. The concentrations of the compound in the organic and aqueous phases were then determined using UV-vis. Log*P* was defined as the logarithm of the ratio of the concentrations of the compound in the organic and aqueous phases (Values reported are the means of three separate determinations).

Subcellular Localization: A549 cells were seeded in 35 mm dishes for 24 h and then incubated with MTDR (500 nM) at 37 °C for 30 min, LTRD (75 nM) at 37 °C for 60 min. The cells were further co-incubated with complexes (1.0 \times IC₅₀) at 37 °C for 2 h. Cells were washed three times with ice-cold PBS and visualized by confocal microscopy (LSM/880NLO) immediately. Complexes were excited at 405 nm, MTDR was excited at 644 nm, LTRD was excited at 594 nm.

Emission was collected at 420-500 nm (Complexes), 660-720 nm (MTDR), 600-660 nm (LTRD).

AO Staining: A549 cells seeded into six-well plate (Corning) were exposed to complexes at the indicated concentrations for 2 h. The cells were then washed twice with PBS and incubated with AO (5 μ M) at 37 °C for 15 min. The cells were washed twice with PBS and visualized by confocal microscopy (LSM/880NLO). Emission was collected at 510 \pm 20 nm (green) and 625 \pm 20 nm (red) upon excitation at 488 nm.

Cellular Uptake Studies: A549 cells were seeded in 35 mm dishes for 24 h and at 4 °C or preincubated with CCCP (10 μ M) or chloroquine (50 μ M) for 2 h. The medium was removed and the cells were then incubated with complexes (1.0 \times IC₅₀) for 15 min. The cells were washed three times with ice-cold PBS and visualize by confocal microscopy (LSM/880NLO) immediately.

Induction of Apoptosis: Flow cytometry analysis of apoptotic populations of the cells caused by exposure to complexes was carried out using the Annexin V-FITC Apoptosis Detection Kit (Beyotime Institute of Biotechnology, China) according to the supplier's instructions. Briefly, A549 cancer cells (1.5 \times 10⁶/2 mL per well) were seeded in a six-well plate. Cells were preincubated in drug-free media at 310 K for 24 h, after which complexes was added at concentrations of 1.0 \times IC₅₀, 2.0 \times IC₅₀ and 3.0 \times IC₅₀ of complexes against A549 cells. After 24 h of drug exposure, cells were collected, washed once with PBS, and resuspended in 195 μ L of annexin V-FITC binding buffer which was then added to 5 μ L of annexin V-FITC and 10 μ L of PI, and then incubated at room temperature in the dark for 15 min. Subsequently, the buffer placed in an ice bath in the dark. The samples were analyzed by a flow cytometer (ACEA NovoCyte, Hangzhou, China).

Cell Cycle Analysis: A549 cells at 1.5 \times 10⁶ per well were seeded in a six-well plate. Cells were preincubated in drug-free media at 310 K for 24 h, after which complexes were added at concentrations of 0.5 \times IC₅₀, 1.0 \times IC₅₀ and 2.0 \times IC₅₀ against A549 cancer cells. After 24 h of drug exposure, supernatants were removed by suction and cells were washed with PBS. Finally, cells were harvested using trypsin-EDTA and fixed for 24 h using cold 70% ethanol. DNA staining was achieved by resuspending the cell pellets in PBS containing propidium iodide (PI) and RNase. Cell pellets were washed and resuspended in PBS before being analyzed in a flow cytometer (ACEA NovoCyte, Hangzhou, China) using excitation of DNA-bound PI at 488 nm, with emission at 585 nm. Data were processed using NovoExpress™ software. The cell cycle distribution is shown as the percentage of cells containing G₀/G₁, S and G₂/M DNA as identified by propidium iodide staining.

Mitochondrial Membrane Assay: Analysis of the changes of mitochondrial potential in cells after exposure to complexes was carried out using the mitochondrial membrane potential assay kit

with JC-1 (Beyotime Institute of Biotechnology, Shanghai, China) according to the manufacturer's instructions. Briefly, 1.5×10^6 A549 cancer cells were seeded in six-well plates left to incubate for 24 h in drug-free medium at 310 K in a humidified atmosphere. Drug solutions, at concentrations of $0.25 \times IC_{50}$, $0.5 \times IC_{50}$, $1.0 \times IC_{50}$ and $2.0 \times IC_{50}$ of complexes against A549 cancer cells, were added in triplicate, and the cells were left to incubate for a further 24 h under similar conditions. Supernatants were removed by suction, and each well was washed with PBS before detaching the cells using trypsin-EDTA. Staining of the samples was done in flow cytometry tubes protected from light, incubating for 30 min at ambient temperature. The samples were immediately analyzed by a flow cytometer (ACEA NovoCyte, Hangzhou, China). For positive controls, the cells were exposed to carbonyl cyanide 3-chlorophenylhydrazone, CCCP ($5 \mu\text{M}$), for 20 min. Data were processed using NovoExpress™ software.

ROS Determination: Flow cytometry analysis of ROS generation in the cells caused by exposure to complexes was carried out using the Reactive Oxygen Species Assay Kit (Beyotime Institute of Biotechnology, Shanghai, China) according to the supplier's instructions. Briefly, 1.5×10^6 A549 cells per well were seeded in a six-well plate. Cells were preincubated in drug-free media at 310 K for 24 h in a 5% CO_2 humidified atmosphere, and then complexes were added at concentrations of $0.25 \times IC_{50}$ and $0.5 \times IC_{50}$ against A549 cells. After 24 h of exposure, cells were washed twice with PBS and then incubated with the DCFH-DA probe ($10 \mu\text{M}$) at 37°C for 30 min, and then washed triple immediately with PBS. The fluorescence intensity was analyzed by flow cytometry (ACEA NovoCyte, Hangzhou, China). Data were processed using NovoExpress™ software. At all times, samples were kept under dark conditions to avoid light-induced ROS production.

Reaction with NADH: The reaction of complexes (ca. $1.0 \mu\text{M}$) with NADH ($100 \mu\text{M}$) in 10% $\text{CH}_3\text{OH}/90\% \text{H}_2\text{O}$ (*v/v*) was monitored by UV-vis at 298 K after various time intervals. TON was calculated from the difference in NADH concentration after 8 h divided by the concentration of ruthenium catalyst. The concentration of NADH was obtained using the extinction coefficient $\epsilon_{339} = 6220 \text{ M}^{-1}\text{cm}^{-1}$.

BSA Binding Experiments: The titration experiments including UV-vis absorption and fluorescence quenching were performed at constant concentration of BSA. A BSA stock solution was prepared in Tris buffer (5 mM Tris-HCl/10 mM NaCl at pH 7.2) and stored at 4°C . All spectra were recorded after each successive addition of the compounds and incubation at room temperature for 5 min to complete the interaction. Target complex was added to both sample cuvette and the reference cuvette in order to offset the self-absorption of complex in the UV region, and working concentration of DMSO was 0.1%~1% (*v/v*). The fluorescence emission spectra of BSA in the absence and presence of complex were recorded with excitation at 285 nm.

In the UV-vis absorption titration experiment, a BSA solution (2.5 mL, 5.0×10^{-6} M) was titrated by successive additions of the stock solutions of complex (1.0×10^{-3} M) and the changes in the BSA absorption were recorded after each addition. Synchronous fluorescence spectra of BSA with concentrations of complex (0-10 μ M) were obtained from 240 nm to 500 nm when $\Delta\lambda = 60$ nm and from 240 to 500 nm when $\Delta\lambda = 15$ nm. The possible fluorescence quenching mechanism was analyzed using the Stern-Volmer equation:

$$F_0/F = 1 + K_{sv} [Q] = 1 + K_q \tau_0 [Q] \quad (1)$$

where, F_0 and F are the fluorescence intensities of BSA in the absence and in the presence of compound $[Q]$, respectively; K_{sv} is the Stern-Volmer quenching constant, K_q is the quenching rate constant and τ_0 is the average lifetime of the fluorophore in the absence of the quencher (10^{-8} s). From the Figure S10, it is possible to calculate K_{sv} values employing *equation 1*, from which K_q can be obtained. The binding constant K_b and number of complex bound to BSA (n) are calculated, using the following formula.

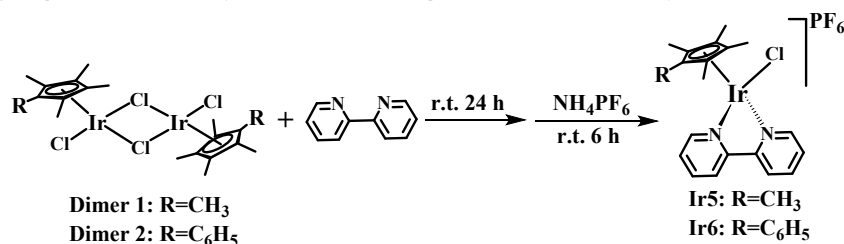
$$\log[(F_0-F)/F] = \log K_b + n \log [Q] \quad (2)$$

Synthesis of $[(\eta^5\text{-C}_5\text{Me}_5)\text{IrCl}_2]_2$ (Dimer 1) and $[(\eta^5\text{-C}_5\text{Me}_4\text{C}_6\text{H}_5)\text{IrCl}_2]_2$ (Dimer 2).

$\text{IrCl}_3 \cdot 3\text{H}_2\text{O}$ (0.50 g, 1.7 mmol) was dissolved in CH_3OH (20 mL) in a microwave vial, pentamethyl cyclopentadiene (0.69 g, 5.0 mmol) was added and reacted at 127 °C, 400 psi for 30 min in a microwave instrument. The reaction mixture was allowed to cool to ambient temperature and the dark green precipitate was filtered off. The volume of the dark red filtrate was reduced to ca. 15 mL on a rotary evaporator. Upon cooling to ambient temperature, an orange precipitate appeared and was collected by filtration. The product was washed with methanol and diethyl ether, dried in air, and pure Dimer **1** was obtained. Yield: 0.40 g (65%). $^1\text{H NMR}$ (500 MHz, CDCl_3): δ 1.60 (s, $J = 1.4$ Hz, 15H).

Dimer **2** was synthesized using phenyltetramethylcyclopentadiene (0.84 g, 5.0 mmol) and $\text{IrCl}_3 \cdot 3\text{H}_2\text{O}$ (0.50 g, 1.67 mmol) according to the method of Dimer **1**. Yield: 0.37 g (58.5%). $^1\text{H NMR}$ (500 MHz, CDCl_3): δ 7.58 (m, 2H), 7.35 (m, 3H), 1.72 (s, 6H), 1.63 (s, 6H).

Synthesis of $[(\eta^5\text{-C}_5\text{Me}_5)\text{Ir}(\text{biPy})\text{Cl}]$ (Ir5) and $[(\eta^5\text{-C}_5\text{Me}_4\text{C}_6\text{H}_5)\text{Ir}(\text{biPy})\text{Cl}]$ (Ir6)



Scheme S1. Design strategy of iridium(III) complex monomers (**Ir5** and **Ir6**).

The general process is as follows: Dimer of iridium (**1** and **2**, 0.05 mmol), bipyridine (15.6 mg, 0.1 mmol) and ammonium hexafluorophosphate (97.8 mg, 0.6 mmol) were added to 40 mL of Methanol and stirred at ambient temperature overnight under N₂. The solvent was removed under reduced pressure, and added 20 mL dichloromethane, the precipitate (sodium acetate) was removed by filtration. Most of the solvent is concentrated to 2.0 mL in vacuum and kept at -20 °C for 12 h, filtered and washed with cold methanol and diethyl ether. The ¹H NMR and ESI-MS were shown in [Scheme S1](#). The data were listed as follows:

$[(\eta^5\text{-C}_5\text{Me}_5)\text{Ir}(\text{biPy})\text{Cl}]$ (**Ir5**): Yield: 83.6%. ¹H NMR (500 MHz, DMSO) δ 8.99 (d, $J = 5.2$ Hz, 2H), 8.79 (s, 1H), 8.78 (s, 1H), 8.34 (td, $J = 8.0, 1.3$ Hz, 2H), 7.88 – 7.85 (m, 2H), 1.67 (s, 15H). ESI-MS (m/z): Calcd for C₂₀H₂₃ClF₆IrN₂P: 664.1; Found 519.1 [M-PF₆]⁺.

$[(\eta^5\text{-C}_5\text{Me}_4\text{C}_6\text{H}_5)\text{Ir}(\text{biPy})\text{Cl}]$ (**Ir6**): Yield: 76.5%. ¹H NMR (500 MHz, DMSO) δ 8.83 (d, $J = 8.1$ Hz, 2H), 8.70 (d, $J = 5.4$ Hz, 2H), 8.35 (t, $J = 7.8$ Hz, 2H), 7.81 (t, $J = 6.6$ Hz, 2H), 7.50 (t, $J = 5.7$ Hz, 5H), 1.77 (s, 6H), 1.68 (s, 6H). ESI-MS (m/z): Calcd for C₂₅H₂₅ClF₆IrN₂P: 726.1; Found 581.2 [M-PF₆]⁺.

2. Figures and tables

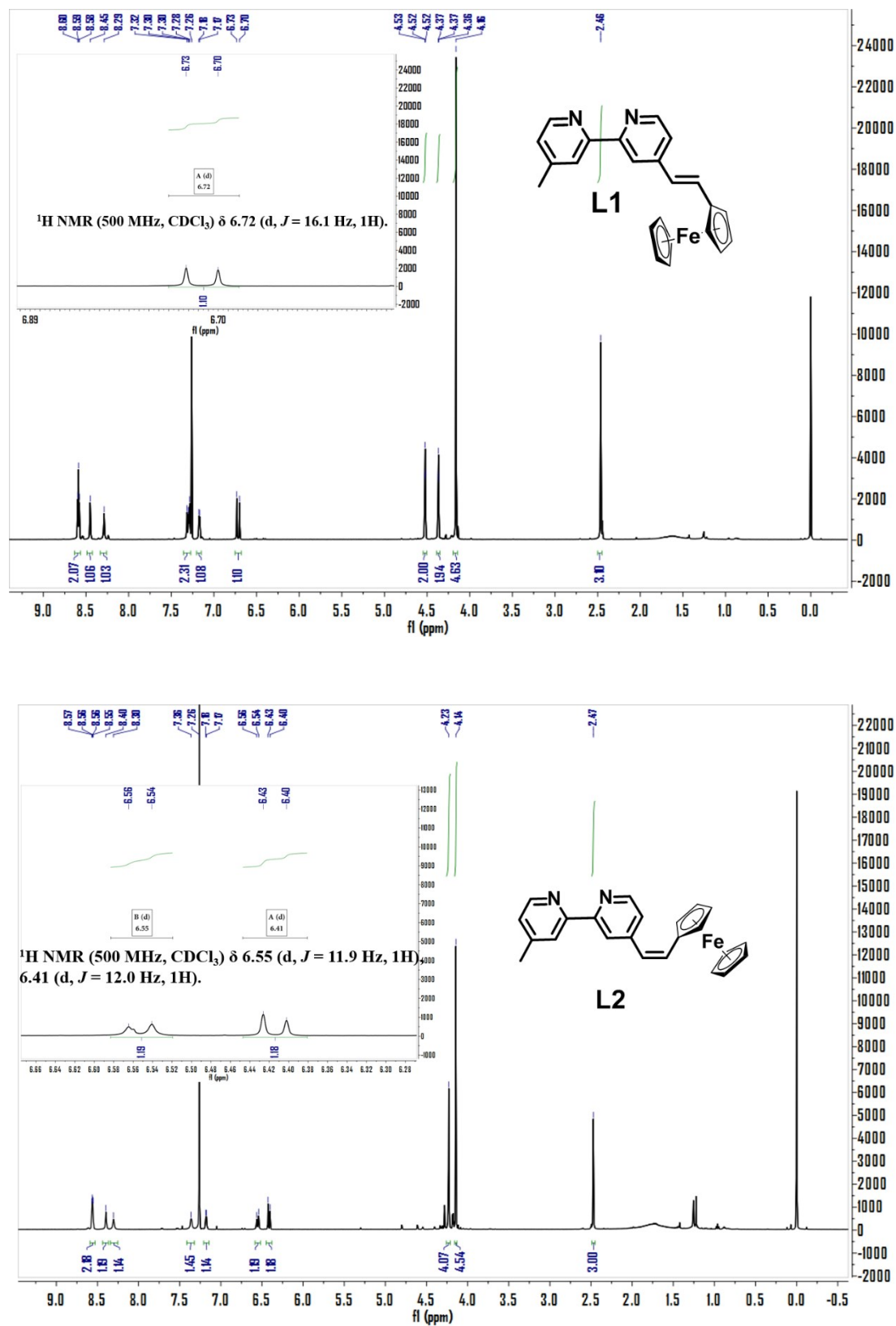


Figure S1. $^1\text{H NMR}$ spectra of L1 and L2 in CDCl_3 .

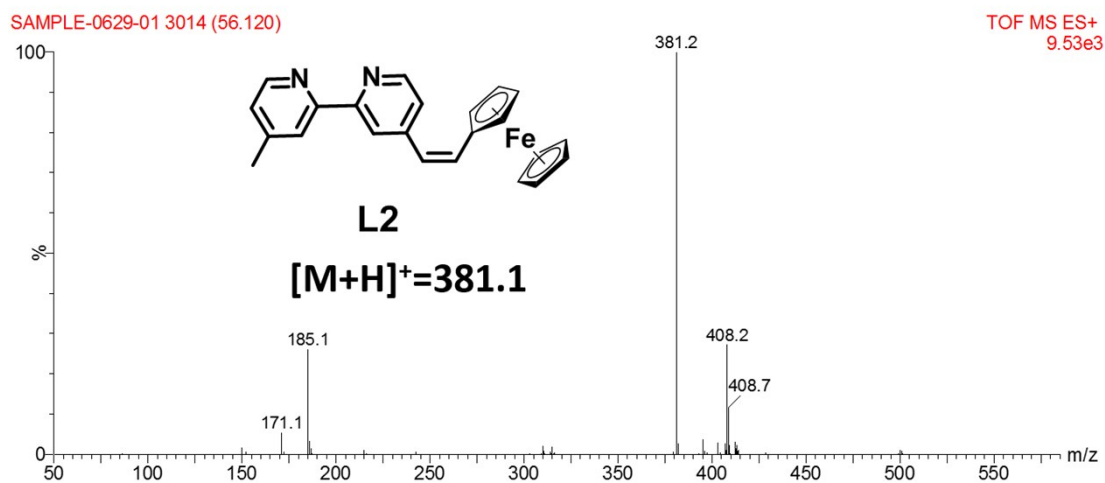
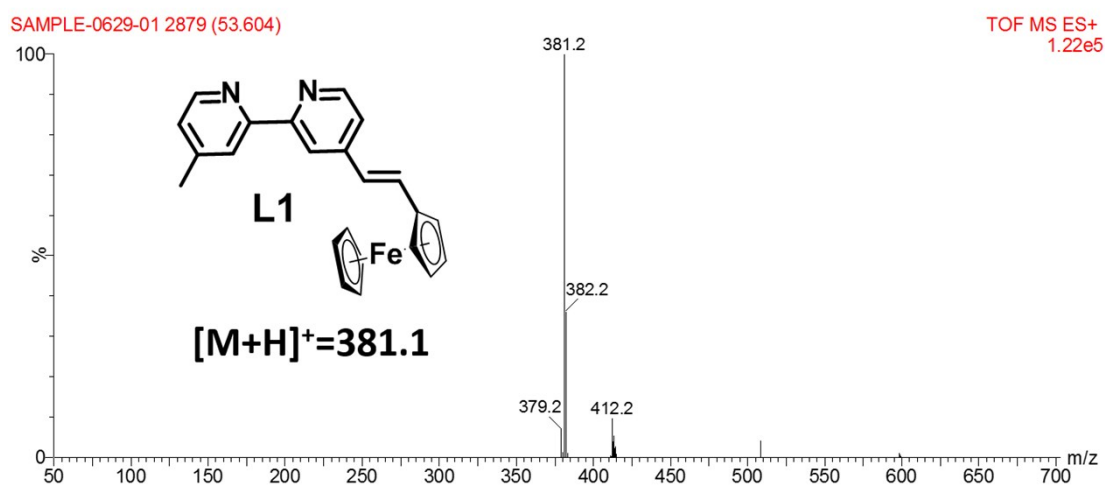
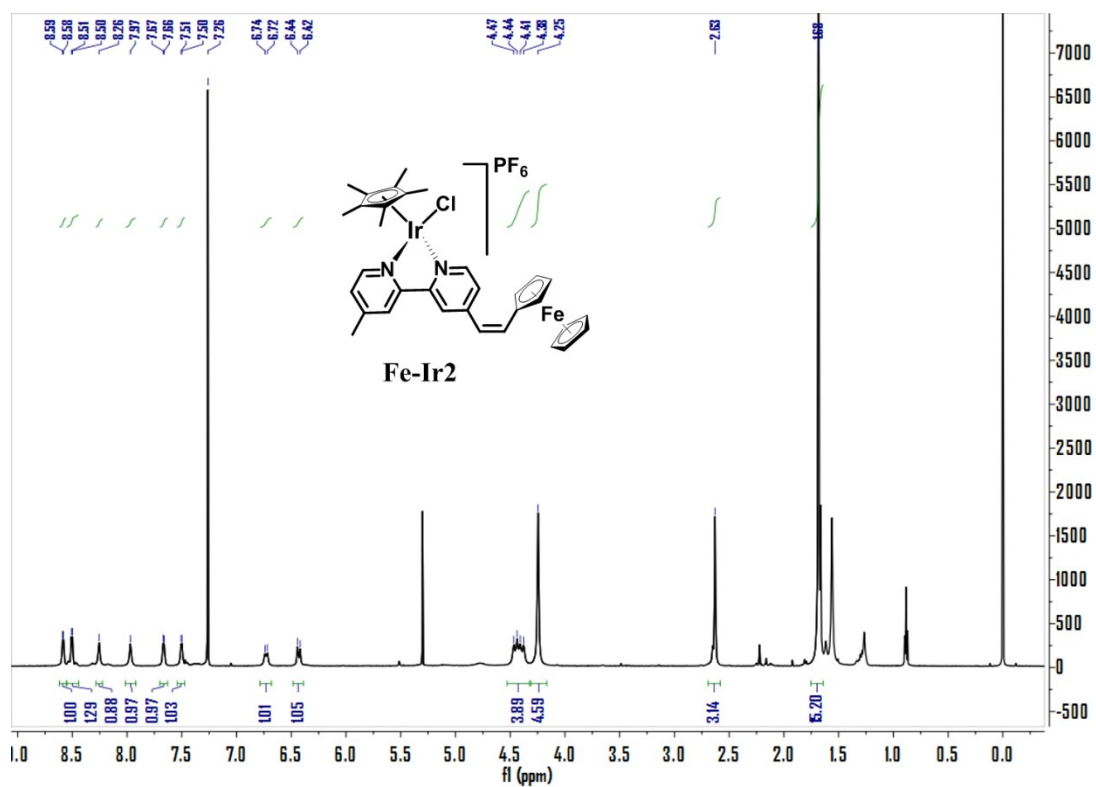
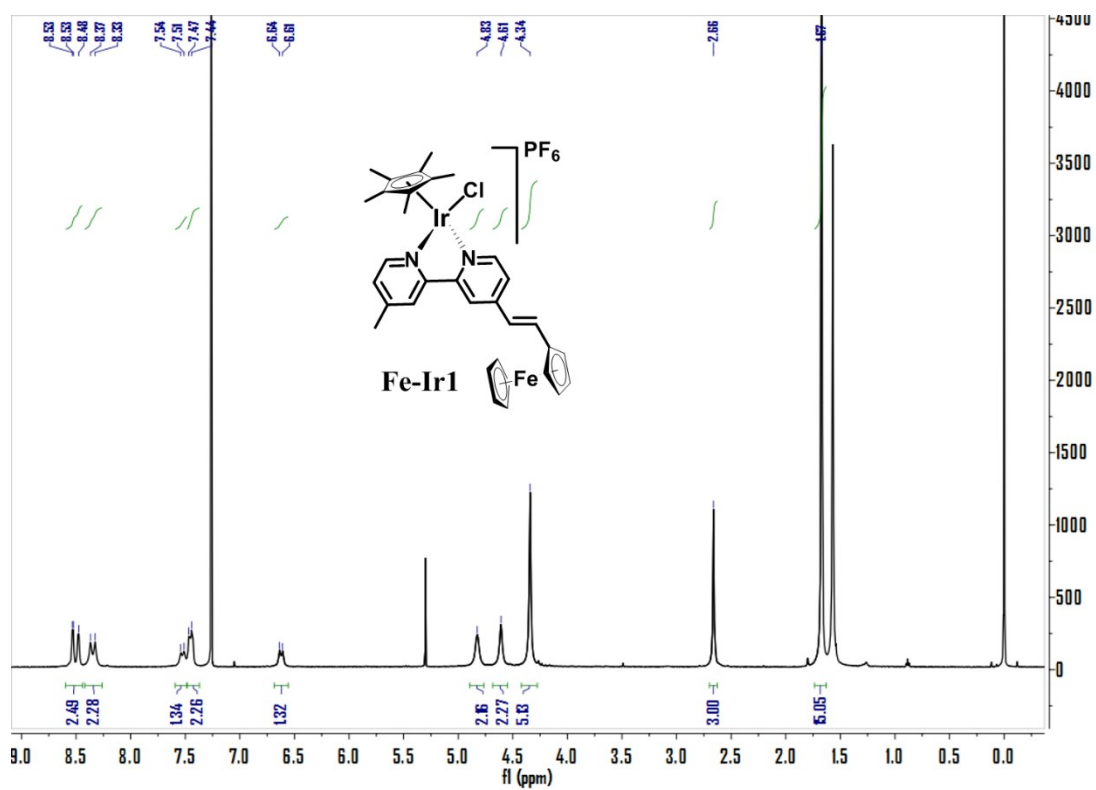


Figure S2. ESI-MS of of ferrocene-modified bipyridine pro-ligands (**L1** and **L2**).



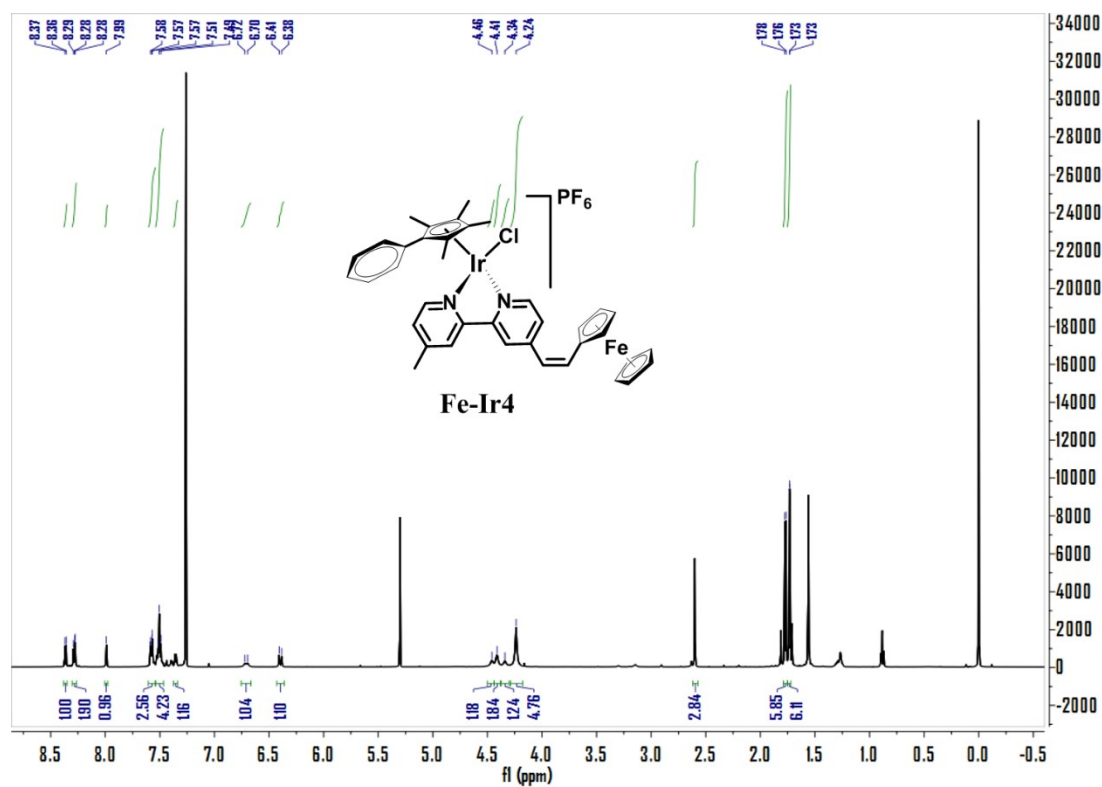
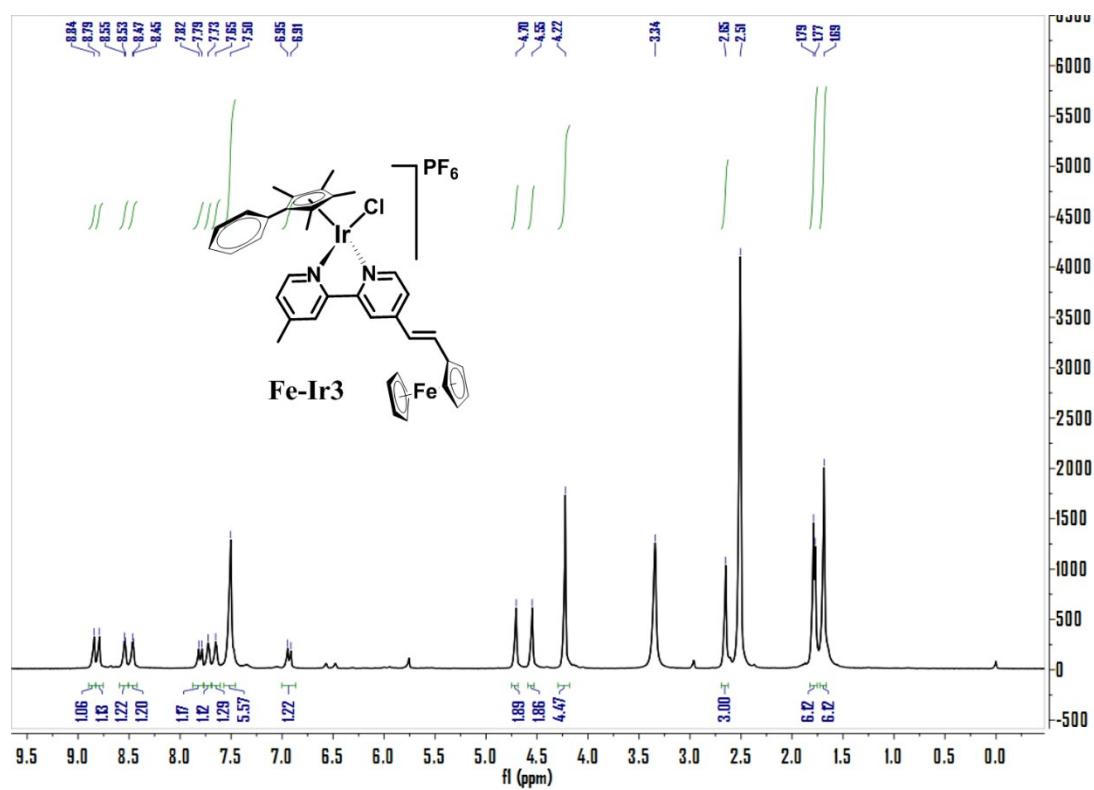
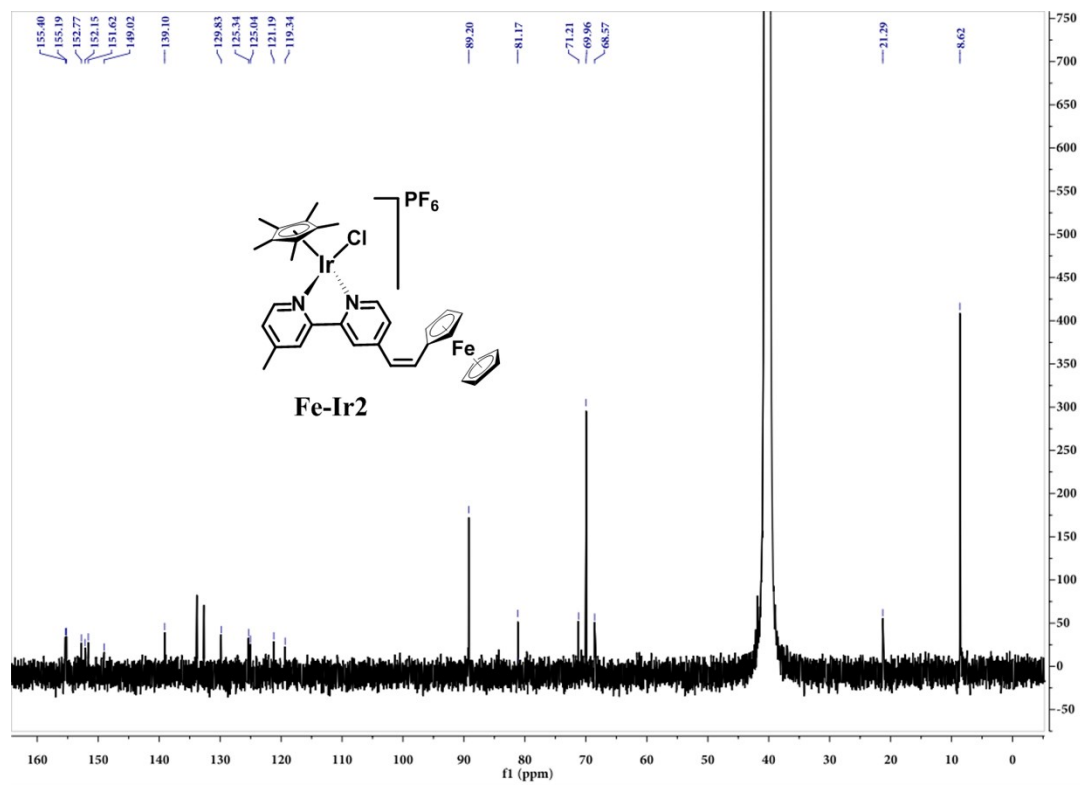
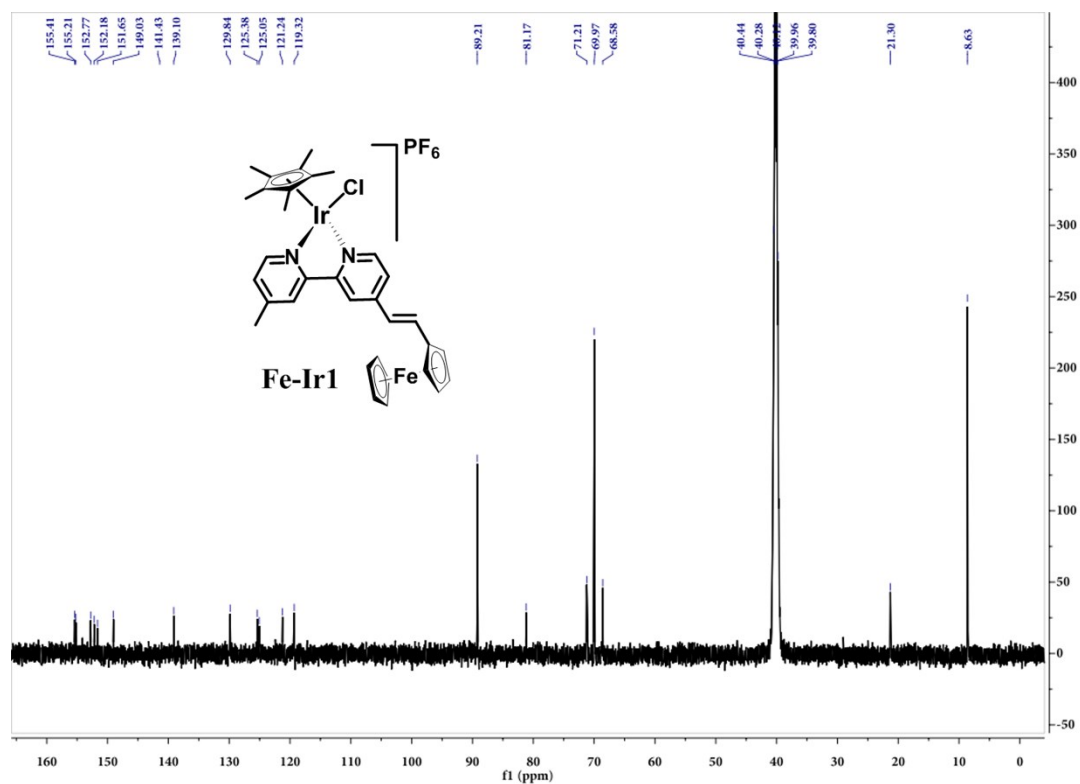


Figure S3. ^1H NMR spectra of Fe(II)-Ir(III) heteronuclear metal complexes in $\text{CDCl}_3/\text{DMSO}$.



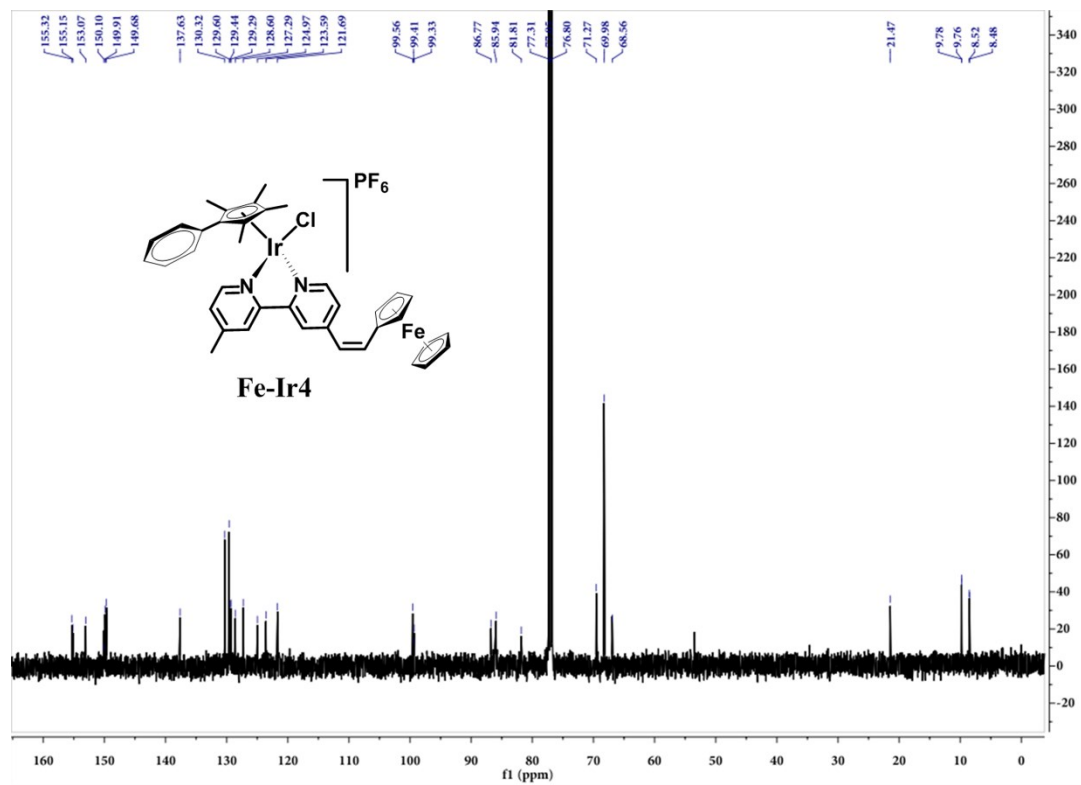
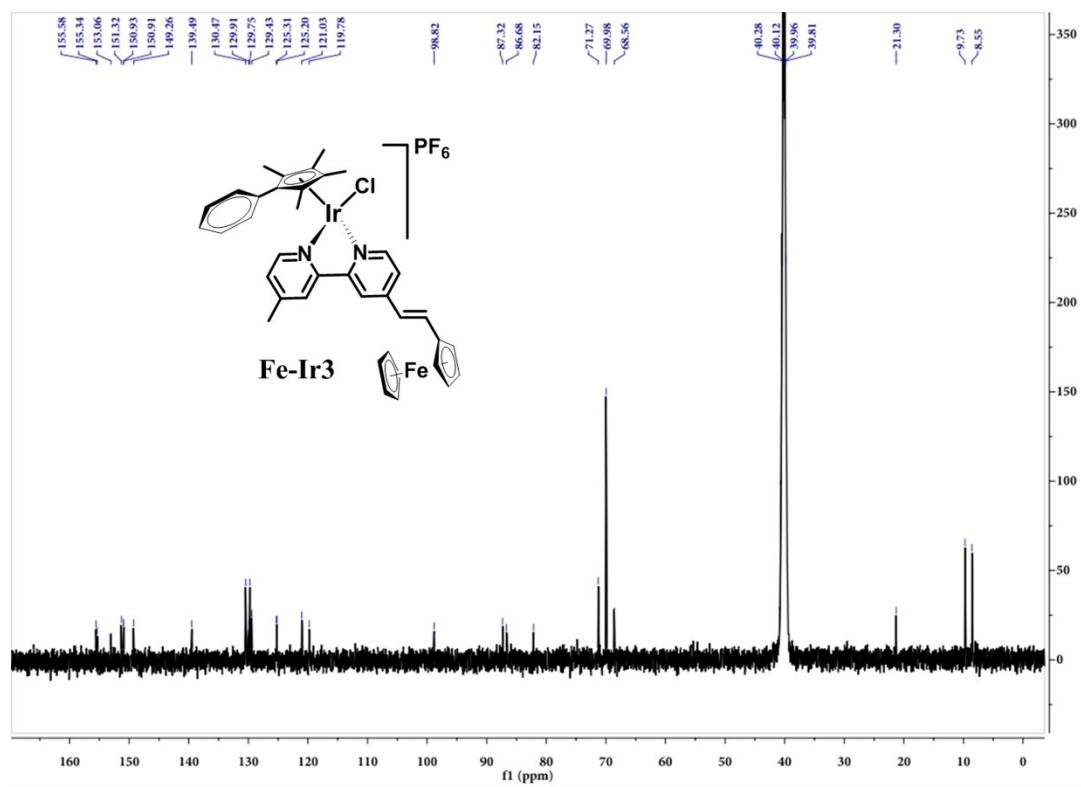
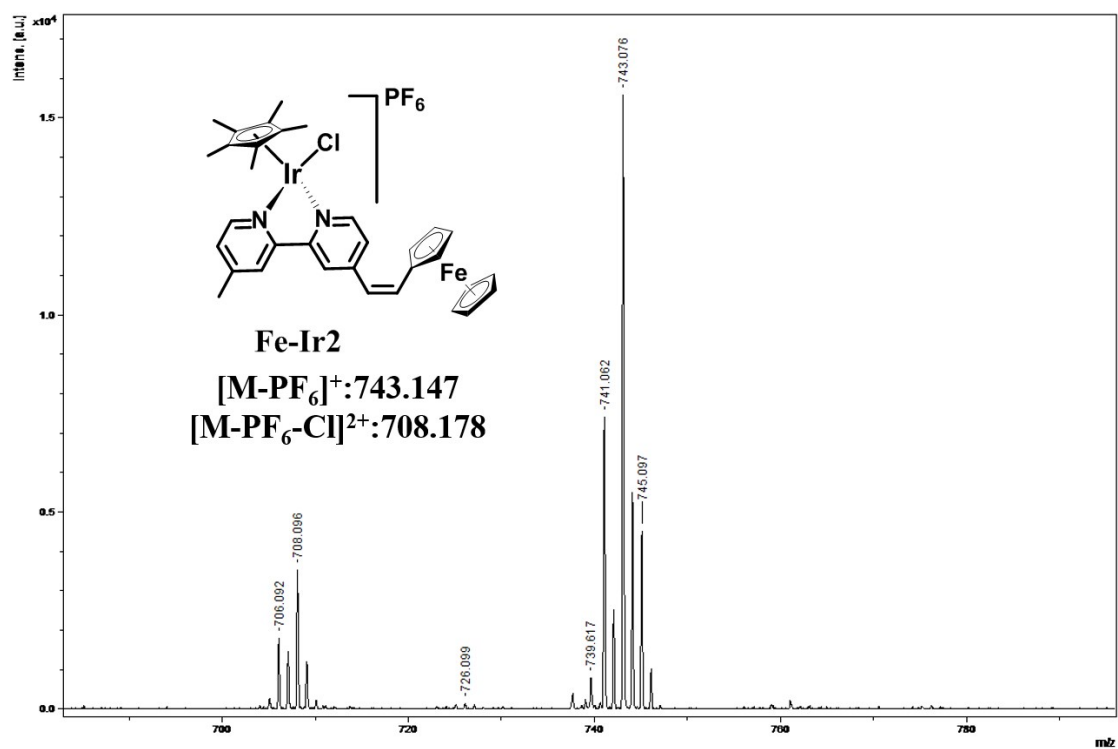
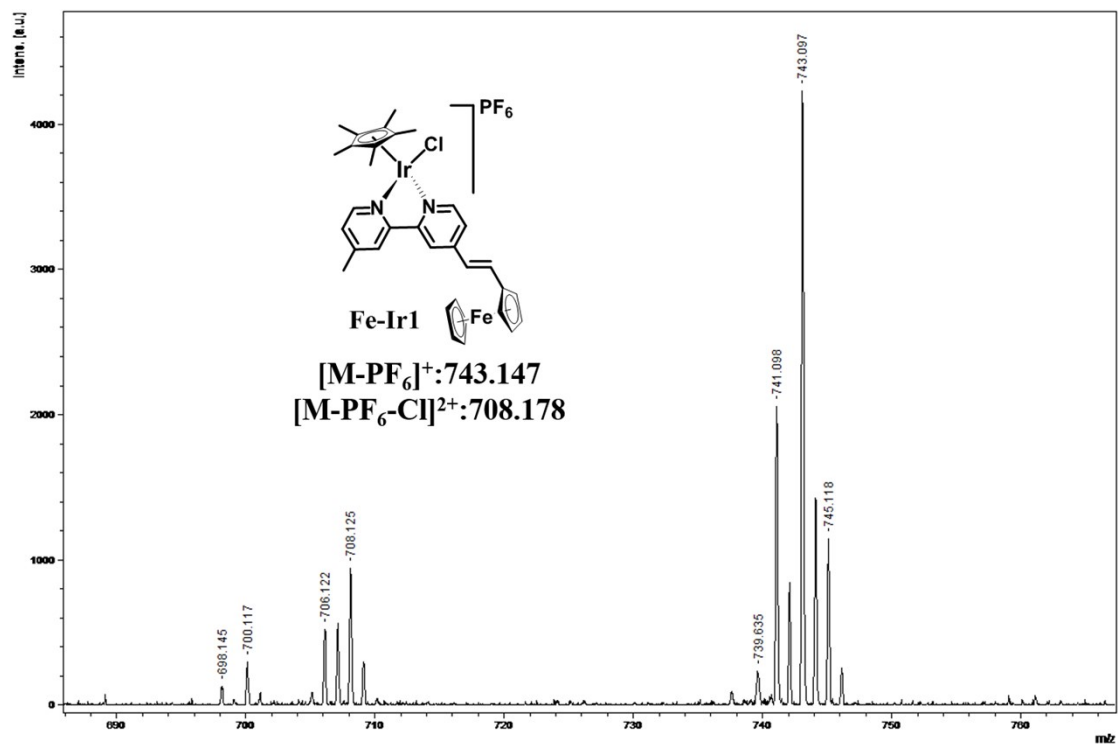


Figure S4 ^{13}C NMR spectra of Fe(II)-Ir(III) heteronuclear metal complexes in $\text{CDCl}_3/\text{DMSO}$.



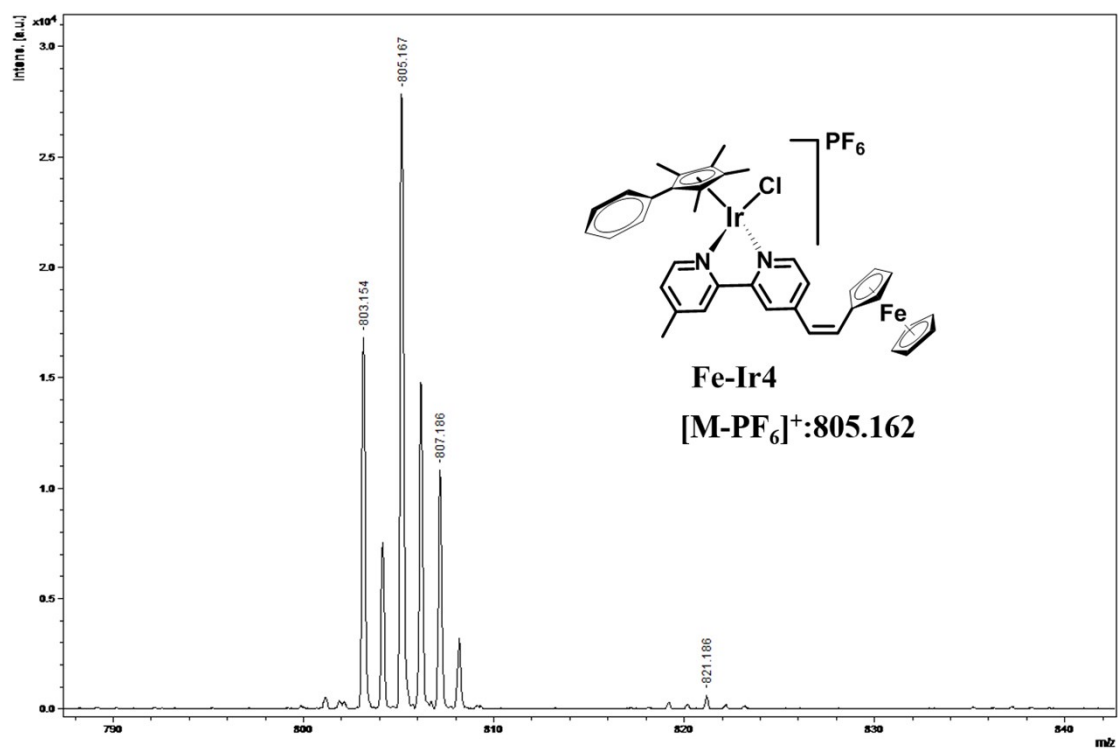
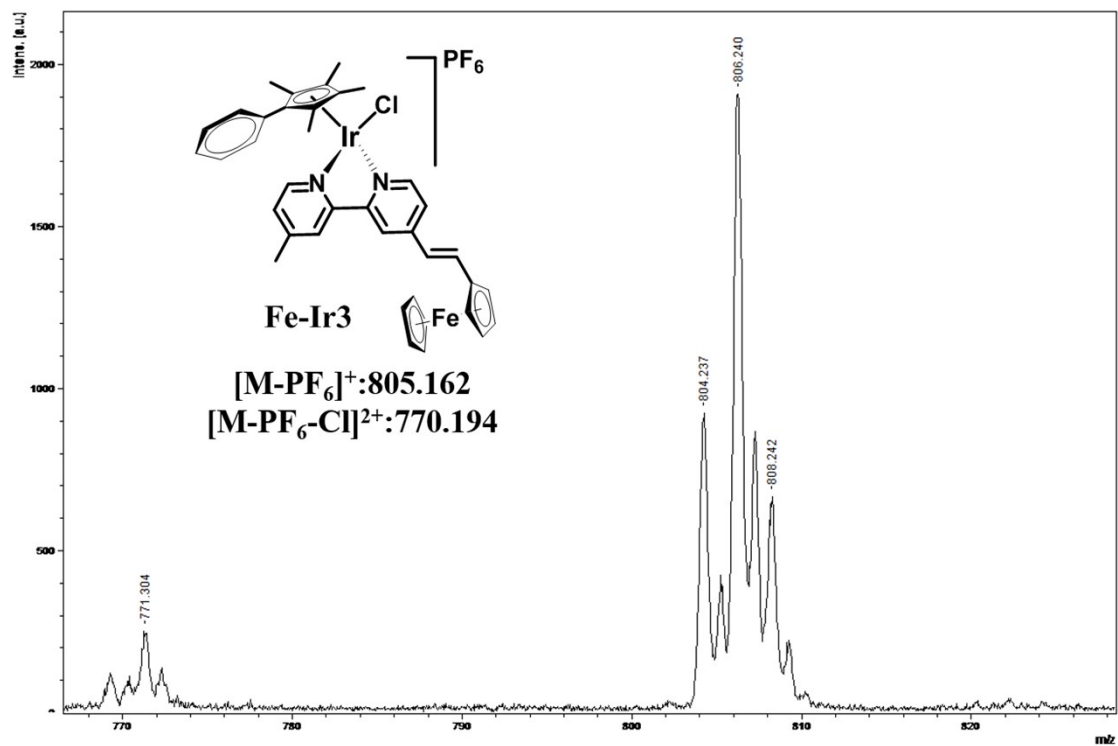


Figure S5. ESI-MS of Fe(II)-Ir(III) heteronuclear metal complexes.

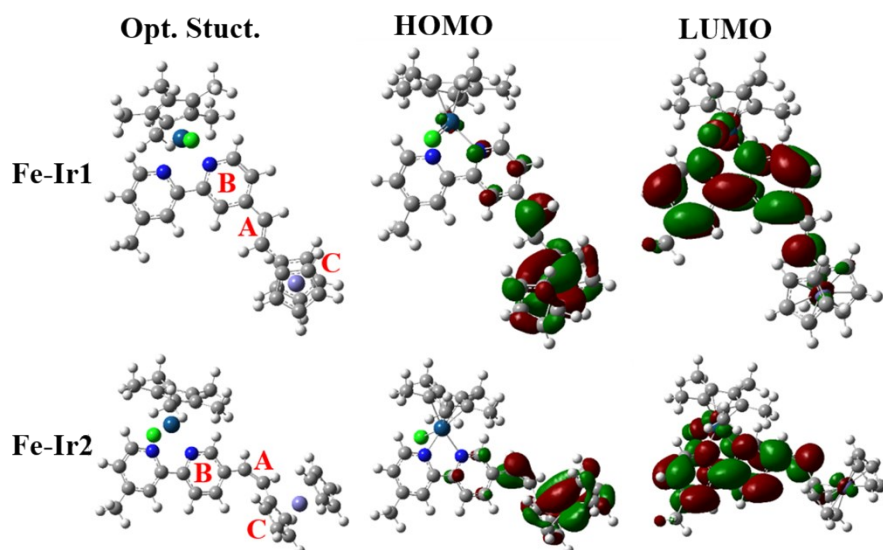


Figure S6. Optimized configuration and electron cloud configuration of frontier molecular orbitals (HOMO and LUMO) of **Fe-Ir1** and **Fe-Ir2**.

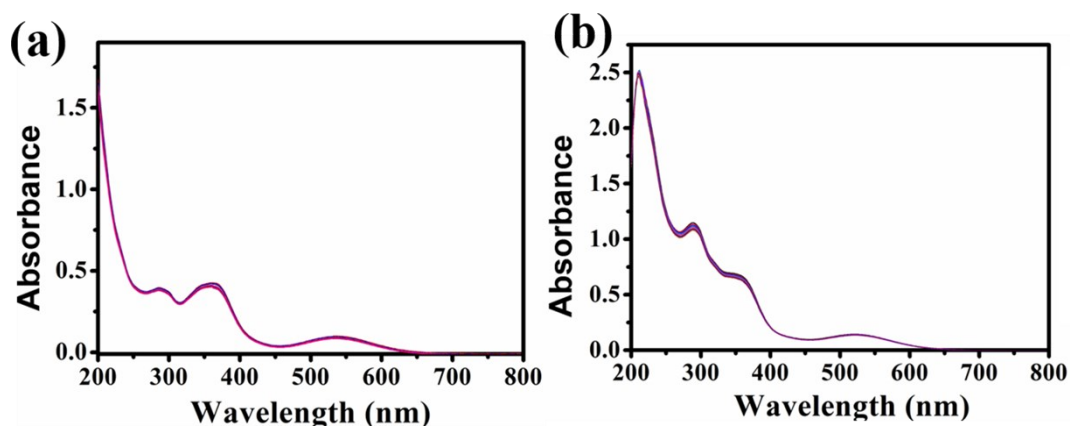


Figure S7. Hydrolysis of **Fe-Ir3** (a) and **Fe-Ir4** (b) in 20% $\text{CH}_3\text{OH}/80\% \text{H}_2\text{O}$ (v/v) at 298 K recorded by UV-vis over a period of 8 h.

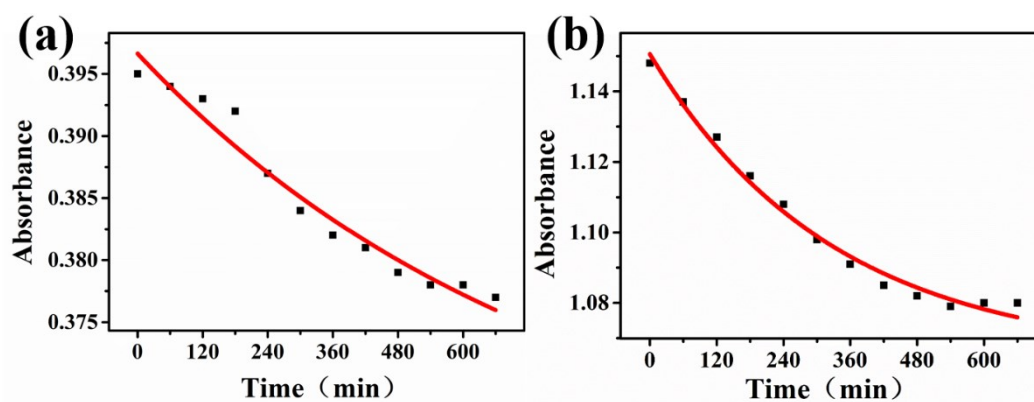


Figure S8. Time dependence of hydrolysis of **Fe-Ir3** (a) and **Fe-Ir4** (b) in 20% $\text{MeOH}/80\% \text{H}_2\text{O}$ (v/v) at 298 K based on UV-vis spectra by measuring the absorption difference.

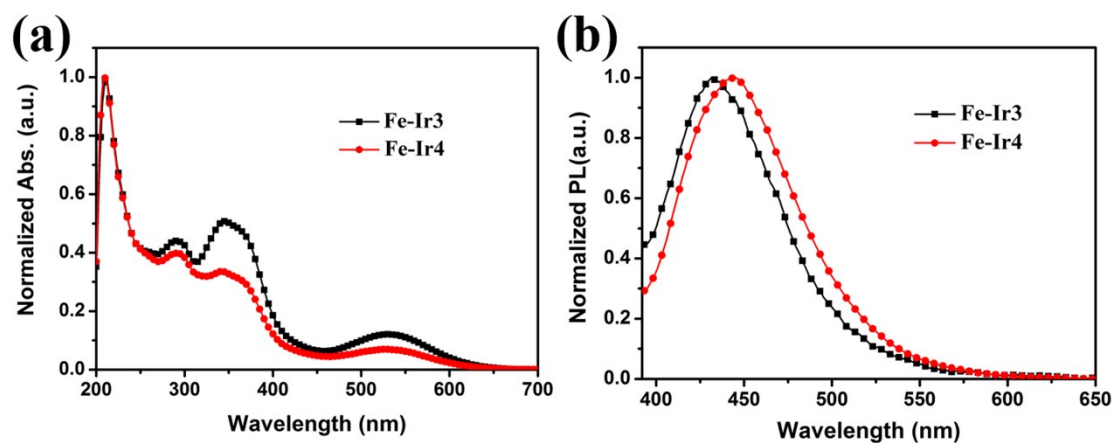


Figure S9. UV-vis spectra (a) and fluorescence spectra (b) of **Fe-Ir3** and **Fe-Ir4** ($20 \mu\text{M}$) in DMSO solution.

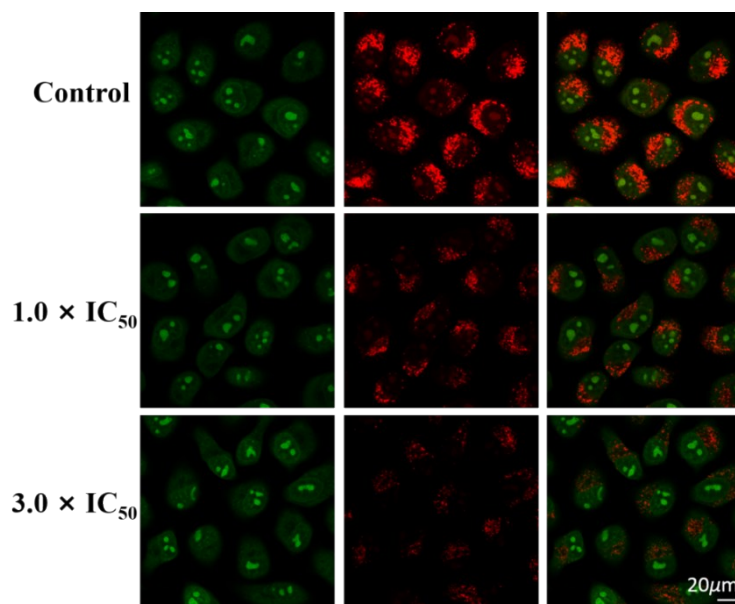


Figure S10. Lysosomal damage in A549 cells caused by **Fe-Ir3** with AO ($5.0 \mu\text{M}$) staining at 37°C for 15 min. Emission was collected at $510 \pm 20 \text{ nm}$ (green) and $625 \pm 20 \text{ nm}$ (red) upon excitation at 488 nm . Scale bar: $20 \mu\text{m}$.

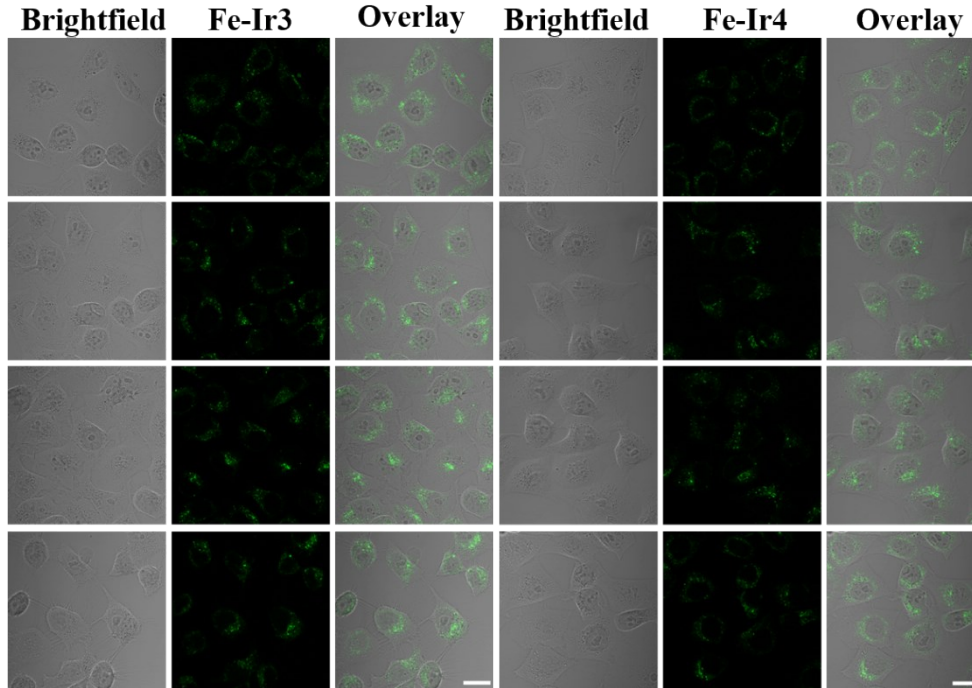


Figure S11. Confocal images of A549 cells after hatched in **Fe-Ir3** and **Fe-Ir4** ($1.0 \times IC_{50}$) under different conditions: Control cells without inhibitor at 310 K (First line); 277 K (Second line); exposed to CCCP at 310 K (Third line); addition of chloroquine ($50 \mu M$) at 310 K (Fourth line). Complexes were excited at 405 nm and emission was collected at 420-500 nm. Scale bar: $20 \mu m$.

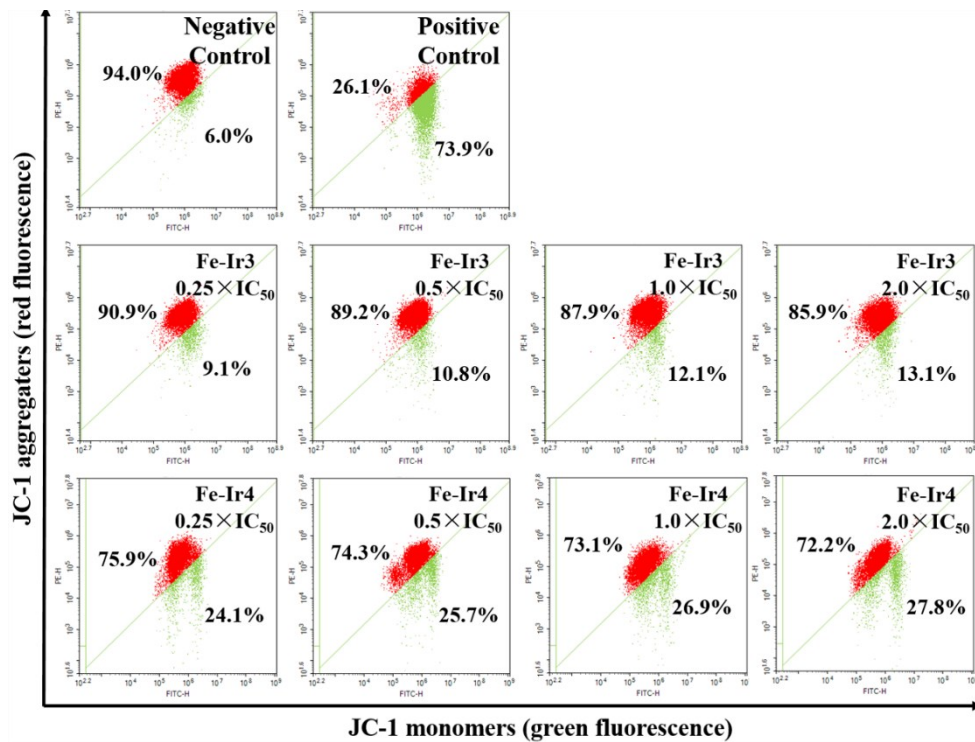


Figure S12. Changes in MMP of A549 cells induced by **Fe-Ir3** and **Fe-Ir4**. Data are quoted as mean \pm SD of two replicates.

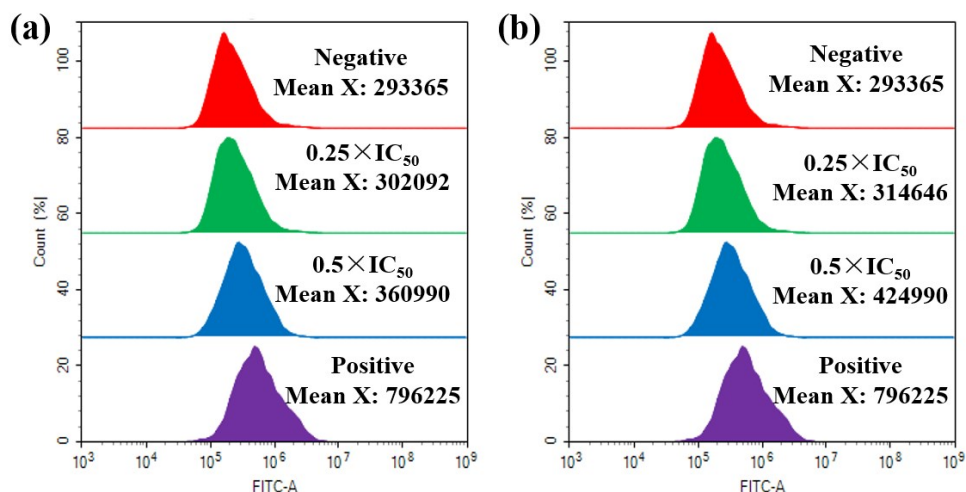


Figure S13. Effect of **Fe-Ir3** (a) and **Fe-Ir4** (b) on intracellular ROS levels in A549 cells treated at the indicated concentrations for 24 h.

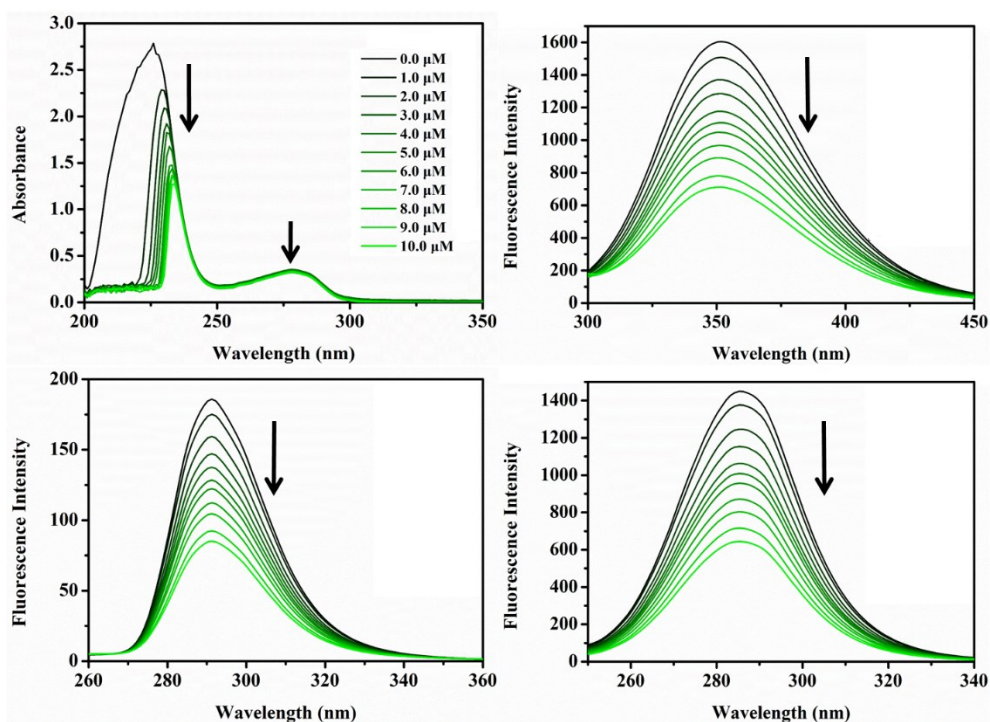


Figure S14. (a) UV-vis spectra of BSA in 5 mM Tris-HCl/10 mM NaCl buffer solution (pH = 7.2) with the increase of **Fe-Ir4** (0-10 μ M). The arrows show the direction of changes in absorbance; (b) Fluorescence spectra of BSA (5 μ M; $\lambda_{ex} = 280$ nm; $\lambda_{em} = 350$ nm) in the absence and presence of **Fe-Ir4** (0-10 μ M); Synchronous spectra of BSA (5 μ M) in the presence of increasing amounts of **Fe-Ir4** (0-10 μ M) with a wavelength of $\Delta\lambda = 15$ nm (c) and $\Delta\lambda = 60$ nm (d).

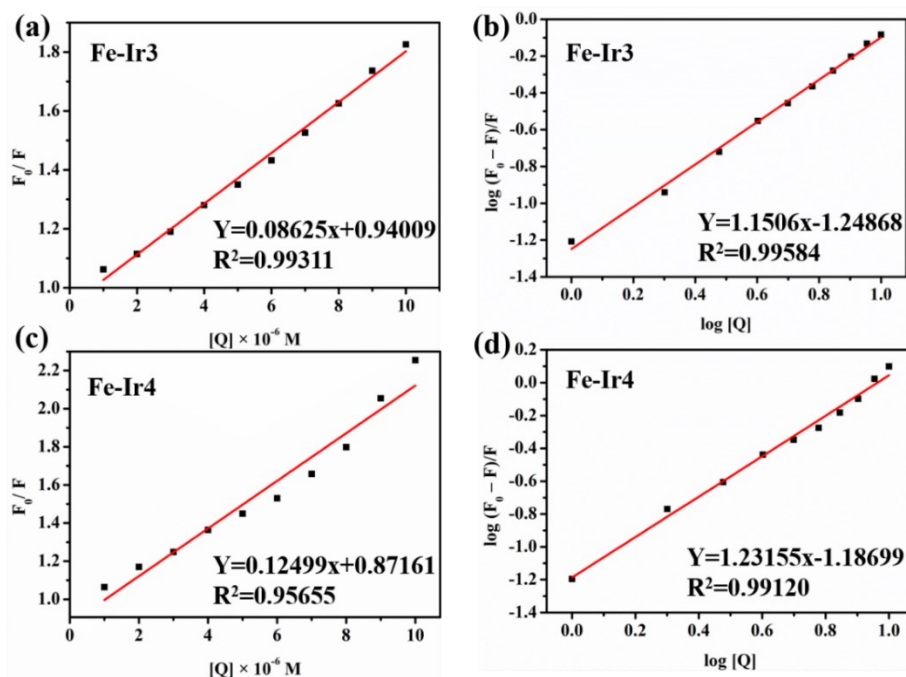


Figure S15. Stern-Volmer plots of F_0/F against **Fe-Ir3** (a) and **Fe-Ir4** (c); Plot of $\log[(F_0-F)/F]$ vs $\log[Q]$ of **Fe-Ir3** (b) and **Fe-Ir4** (d).

Table S1. Crystallographic data and structure refinement for **Fe-Ir1**.

Empirical formula	$C_{33}H_{35}N_2ClF_6PF_6Ir$	Density (mg/m^3)	1.671
Formula weight	888.10	Z	4
Temperature (K)	295(2)	Absorption coefficient (mm^{-1})	4.354
Crystal color	Reddish brown	F(000)	1744
Cryst size (mm)	0.32×0.26×0.20	Volume (\AA^3)	3530.0(7)
Wavelength (\AA)	0.71073	Theta range for data collection (deg)	1.44 to 26.00
Crystal system	Monoclinic	Limiting indices	$-10 \leq h \leq 9$, $24 \leq k \leq 25$, $23 \leq l \leq 23$
Space group	P21/c	Reflections collected/unique	18872/6924 [R(int) = 0.0241]
a (\AA)	8.8471(10)	Completeness to theta = 26.00 (%)	99.9
b (\AA)	20.875(2)	Max./min. transmission	0.4763/0.3363
c (\AA)	19.174(2)	Data/restraints/parameters	6924/0/412
α ($^\circ$)	90	Goodness-of-fit on F^2	1.082
β ($^\circ$)	94.529(2)	Final R indices [I>2 σ (I)]	R1=0.0351, wR2=0.1039
γ ($^\circ$)	90	R indices (all data)	R1=0.0430, wR2=0.1090

Table S2. Selected bond lengths (Å) and angles (deg) for **Fe-Ir1**.

Sn(1)-C(13)	2.134(2)
Sn(1)-C(1)	2.144(2)
Sn(1)-C(7)	2.142(3)
Sn(1)-C(19)	2.153(2)
N(1)-N(2)	1.382(3)
N(2)-C(22)	1.272(3)
C(21)-O(1)	1.231(3)
C(13)-Sn(1)-C(1)	105.66(9)
C(13)-Sn(1)-C(7)	102.67(10)
C(1)-Sn(1)-C(7)	107.61(9)
C(13)-Sn(1)-C(19)	114.47(9)
C(1)-Sn(1)-C(19)	117.20(10)
C(7)-Sn(1)-C(19)	108.10(9)

Table S3. Selected angles for **Fe-Ir1** and **Fe-Ir2**.

	$\theta(^{\circ})$		
	A-B	B-C	A-C
Fe-Ir1	0.559/4.175*	0.120/0.411*	0.990/3.840*
Fe-Ir2	13.874	18.807	43.482

Footnotes: **A**, **B** and **C** represent pyridine attached to olefin, olefin and cyclopentadiene ring attached to olefin (Figure S4); *: the corresponding data of crystal.

Table S4. Flow cytometry analysis to determine the percentages of apoptotic cells, using Annexin V-FITC/PI staining, after exposing A549 cells to **Fe-Ir3**.

Concentration	Population (%)			
	Viable	Early apoptosis	Late apoptosis	Non-viable
Control	94.4±0.2	2.2±0.5	3.0±0.1	0.4±0.1
1.0 × IC ₅₀	82.1±0.9	1.9±0.2	15.6±0.7	0.4±0.03
Fe-Ir3	78.6±3.3	3.3±0.3	17.7±2.0	0.4±0.07
3.0 × IC ₅₀	78.6±3.3	3.3±0.3	17.7±2.0	0.4±0.07

Table S5. Flow cytometry analysis to determine the percentages of apoptotic cells, using Annexin V-FITC/PI staining, after exposing A549 cells to **Fe-Ir4**.

Concentration	Population (%)			
	Viable	Early apoptosis	Late apoptosis	Non-viable
Control	94.6±0.6	1.9±0.4	3.5±0.3	0.1±0.04
1.0 × IC ₅₀	74.5±1.9	3.2±0.2	21.3±1.8	1.0±0.2
Fe-Ir4	69.0±1.3	4.3±0.4	26.5±0.2	0.2±0.1

3.0 × IC₅₀ 65.3±1.3 3.7±0.9 30.1±0.9 0.9±0.4

Table S6. Cell cycle analysis carried out by flow cytometry using PI staining after exposing A549 cells to **Fe-Ir3**.

Concentration	Population(%)			
	G ₀ /G ₁ phase	S phase	G ₂ /M phase	Sub-G1 phase
Control	69.3±0.1	23.8±0.5	13.7±2.3	0.1
0.5 × IC ₅₀	64.9±2.7	23.1±0.8	14.1±1.3	0.2
Fe-Ir3	65.9±0.7	24.9±0.4	16.1±0.8	1.1±0.4
2.0 × IC ₅₀	61.2±1.3	26.9±0.1	16.0±0.7	2.1±0.9

Table S7. Cell cycle analysis carried out by flow cytometry using PI staining after exposing A549 cells to **Fe-Ir4**.

Concentration	Population(%)			
	G ₀ /G ₁ phase	S phase	G ₂ /M phase	Sub-G1 phase
Control	60.5±1.7	29.9±0.2	11.8±0.1	0.2
0.5 × IC ₅₀	57.8±3.1	31.0±1.8	12.9±0.9	0.3
Fe-Ir4	52.8±0.8	36.3±1.7	18.1±0.3	1.1±0.1
2.0 × IC ₅₀	52.9±1.1	28.5±0.1	22.2±1.0	3.2±1.7